

Spark Ignition Engine Torque Management

Grant A. Ingram¹, Matthew A. Franchek,

Venkataramanan Balakrishnan, and Gopichandra Surnilla[†]

Purdue University (West Lafayette, IN), [†]Ford Motor Company (Dearborn, MI)

Abstract

Presented in this paper is a robust feedback controller design procedure to regulate the torque of a spark ignition engine equipped with an electronic throttle mass air flow controller. To this end, a system level model of engine torque production is experimentally determined. Next, a crank-angle domain H_∞ controller is designed to control engine torque with zero steady state error while addressing the nonlinear system characteristics and pure delay. The controller design methodology applied to the torque control problem is presented and an interpretation of the controller provided. Engine dynamometer data acquired from a Ford 4.6L V8 engine demonstrates the H_∞ controller successfully rejects noise and disturbances while meeting transient and steady state performance objectives.

1 Introduction

Two of the largest challenges for the automotive industry are (1) the improvement of automobile fuel economy and (2) the reduction of emissions. To accomplish these goals, sophisticated automatic engine control strategies must be constructed to ensure proper air/fuel delivery is maintained during all driving scenarios. One method of improving automobile fuel economy while reducing emissions is to implement lean burn technology [1].

Lean burn technology consists of lean engine operation during certain driving modes to improve vehicle fuel economy. An estimated five to six percent increase of fuel economy is anticipated during homogeneous lean operation. The improvement of fuel economy during lean operation is gained from reducing engine pumping losses and improving thermodynamic efficiency.

Lean burn technology typically implements a three-way catalyst that is able to store NO_x (a lean NO_x trap or LNT) during lean operation. Once the catalyst is filled with NO_x , the engine is operated rich to purge NO_x from the LNT and allow lean operation to resume.

During these lean/rich air/fuel transitions, the engine torque should remain relatively constant in order to maintain vehicle drivability. Since the torque of a spark ignition engine varies with air/fuel ratio (AFR), one of the many challenges

implementing lean burn technology is engine torque control.

The objective of this investigation is to design a robust feedback controller to regulate the torque of a 4.6L V8 spark ignition engine equipped with an electronic throttle mass air flow controller. Individual air charge per cylinder is directly related to torque production [2]. Therefore, mass air flow may be commanded to minimize torque variations via an open loop mapping or by the design of an outer loop controller with torque feedback. Torque feedback may be provided by a sensor, however this would be costly. This has led to an increasing amount of literature investigating engine torque estimation algorithms [3, 4]. For this investigation, torque feedback will be provided via the dynamometer load cell. However, this design methodology may also be implemented using an estimate of the engine torque. Beyond torque control for conventional lean burn systems, this work has applications including hybrid automobile engine control, vehicle speed control for intelligent vehicle highway systems, improved stoichiometric fuelling during transients, improved transmission shifts, as well as many others.

The controller design challenges for torque control are three-fold. First, the system contains a pure delay, which must be incorporated in the design. Second, many parameters such as AFR, engine speed, mass air flow, spark, and exhaust gas recirculation (EGR) affect engine torque production. Third, the controller must accommodate a large range of engine operating conditions. To overcome these challenges, a model must be determined by either first principles and/or system identification techniques. It turns out that first-principle models of a spark ignition engine are too unwieldy to be of much use in controller design. Consequently, our modeling efforts were focused on an experimental method of system identification that captures the nonlinear engine torque characteristics for a large range of operating conditions. The model uncertainty must be addressed and requires robust controller design methodologies to guarantee system performance. H_∞ methods are employed for this purpose.

Torque control has been investigated by several researchers: Kamei [5], Kolmanovsky [6], and Balluchi [7] and references therein. However, the controller design methodology presented in this paper is based on the determination of a static torque function, experimental system identifi-

¹corresponding author: gingham@ecn.purdue.edu

cation, and finally a robust H_∞ controller design. In this paper, a 4.6L V8 spark ignition engine torque production system level model is experimentally determined. In addition, an H_∞ controller is designed to control engine torque with zero steady state error while addressing the nonlinear system characteristics and pure delay. A discussion of the controller design methodology applied to the torque control problem and an interpretation of the design is presented. Engine dynamometer data demonstrates the H_∞ controller successfully rejects noise and disturbances while maintaining acceptable performance.

2 Main Results

A robust feedback controller design procedure is presented for the regulation of engine torque. The controller design addresses the following:

1. induction-to-power delay,
2. torque production variations due to: AFR, engine speed, mass air flow, spark, and exhaust gas recirculation (EGR),
3. and a large range of engine operating conditions.

Furthermore, the controller must maintain zero steady state error and provide acceptable transient behavior. The solution presented is broken into two parts, (1) identification of the system including a steady state function of torque production and (2) an H_∞ robust controller design.

2.1 Identification of Dynamic Model

A two part system identification process is employed to determine the control-oriented system model. First, a static (steady-state) function is measured to capture a large majority of engine nonlinearities. Second, a transfer function estimation of the combined system, i.e. the static function and engine, is calculated to develop a dynamic model with uncertainty. To accomplish these goals, experimental data was collected from a Ford 4.6L V8 spark ignition engine and 175 hp eddy current dynamometer using a dSpace data acquisition system. The two part system identification is detailed in the following subsections.

2.1.1 Development of Nonlinear Steady State

Torque Map: Engine torque production is affected by several variables: AFR, engine speed, mass air flow, spark timing, and EGR. For this reason, a linear model alone is not applicable to describe the system dynamics from engine mass air flow to torque production. Therefore, a function representing the relationship between mass air flow, engine speed, and AFR to engine torque in tandem with an uncertain linear model will be developed. For this investigation, EGR and spark timing are not commanded explicitly by the torque controller. The engine control module will actuate these parameters based on normal engine operation. Therefore, for this investigation, EGR and spark timing contribute to the uncertainty of the model.

The development of a static engine map is an important step in linearizing the system. Experimental data was collected sweeping mass air flow for λ (AFR/AFR_{stoich}) values bounded by 0.7 and 1.3. Data was collected at various engine speeds between 800 rpm and 4000 rpm. The forward-regression version of the orthogonal least squares (OLS) estimator was implemented to efficiently determine a polynomial equation describing the relationship between λ , torque, engine speed, and mass air flow. The forward-regression orthogonal procedure selects parameters from a set of possible candidate parameters such that the maximum increment to explained variance is achieved for each additional model parameter. Billings provides a complete description of this procedure [8].

From first principles, torque is proportional to the following [9],

$$Torque \propto \frac{MAF}{RPM \cdot \lambda}. \quad (1)$$

However, engine torque is not significantly affected by $\lambda < 1$ provided λ does not exceed the rich limit of the engine. Engine torque is significantly affected by $\lambda > 1$. Therefore, a nonlinear term, $\hat{\lambda}$, is defined as

$$\hat{\lambda} = \begin{cases} \lambda, & \lambda > 1 \\ 1, & \lambda \leq 1. \end{cases} \quad (2)$$

The nonlinear term, $\hat{\lambda}$, provides another possible model parameter which incorporates more information regarding engine torque production. Possible combinations of torque, engine speed, and λ or $\hat{\lambda}$ will be included in the set of possible candidate parameters for the relationship between λ , torque, engine speed, and mass air flow. The following is a list of possible candidate parameters: *DC term*, λ , λ^2 , λ^3 , *Torque*, $Torque^2$, $Torque^3$, *RPM*, RPM^2 , RPM^3 , $\lambda \cdot Torque$, $\lambda^2 \cdot Torque$, $\lambda \cdot Torque^2$, $\lambda \cdot RPM$, $\lambda^2 \cdot RPM$, $\lambda \cdot RPM^2$, $Torque \cdot RPM$, $Torque^2 \cdot RPM$, $Torque \cdot RPM^2$, $\lambda \cdot Torque \cdot RPM$, $\hat{\lambda}$, $\hat{\lambda}^2$, $\hat{\lambda}^3$, $\hat{\lambda} \cdot Torque$, $\hat{\lambda}^2 \cdot Torque$, $\hat{\lambda} \cdot Torque^2$, $\hat{\lambda} \cdot RPM$, $\hat{\lambda}^2 \cdot RPM$, $\hat{\lambda} \cdot RPM^2$, and $\hat{\lambda} \cdot Torque \cdot RPM$. The forward-regression orthogonal procedure selected model terms from the possible candidate terms to determine the steady state relationship between requested engine mass air flow and engine torque, rpm, and λ . This relationship may be described by

$$MAF_{requested} = \Theta_1 \cdot (Torque \cdot RPM \cdot \hat{\lambda}) + \Theta_2 \cdot (RPM). \quad (3)$$

where Θ_n are the parameters identified by forward-regression OLS. As expected, the first principles relationship from Equation (1) is contained within the polynomial relationship. Equation (3) was validated to ensure a proper mapping was achieved. Now that the static engine torque function has been developed, the identification of the dynamic system may begin.

2.1.2 System Identification of Steady State Torque Function and Engine: A model of the engine dynamics

Table 1: Engine Conditions for Dynamic System Identification.

Speed (mph)	Engine RPM	Torque (ft-lbs)	Lambda (AFR/AFR _{stoich})
~25	1000	78	1.0 and 1.3
~47	1260	110	1.0 and 1.3
~58	1550	155	1.0 and 1.3
~74	2000	142	1.0 and 1.3

related to torque production is required for controller design. So far, a static function has been determined experimentally to remove the majority of the system nonlinearities. Now, the frequency response estimation of the combined system, i.e. the steady state torque function and engine, may commence.

A block diagram of the dynamic system to be identified is shown in Figure 1. White noise was sent as a command input to the steady state torque function denoted by $fn(\cdot)$ in Figure 1 and described in Equation (3). The white noise perturbs the desired torque command while current engine speed and λ are also provided to the steady state torque function. The output of the static torque function provides a command to the mass air flow controller and in turn provides a perturbation signal to the engine. The mass air flow controller and design is discussed by Ingram [10]. Desired and actual engine torque were measured in the crank-angle domain for several engine operating conditions as shown in Table 1. Crank-angle domain measurements were sampled every 90 degrees of crank rotation ($\frac{1}{8}$ of an engine cycle). For clarity, ω_θ and s_θ will denote that frequencies and the Laplace transformation are defined with respect to the crank-angle domain. For more information, crank-angle domain engine dynamics are discussed by Chin [11].

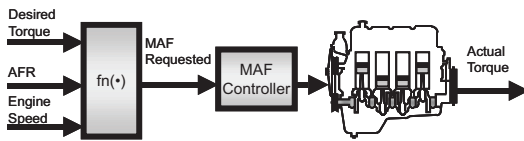


Figure 1: System Identification.

The system was identified implementing a standard frequency response function calculation,

$$H(j\omega_\theta) = \frac{S_{xy}(j\omega_\theta)}{S_{xx}(j\omega_\theta)} \quad (4)$$

where $H(j\omega_\theta)$ is the system frequency response function, $S_{xy}(j\omega_\theta)$ is the cross spectral density of the input and output, and $S_{xx}(j\omega_\theta)$ is the auto spectral density of the input. This calculation is designed to provide an unbiased estimate of a single input/single output system with uncorrelated output noise [12]. For each operating condition shown in Table 1, an experimental frequency response of the system was calculated. The frequency response functions are shown in Figure 2.

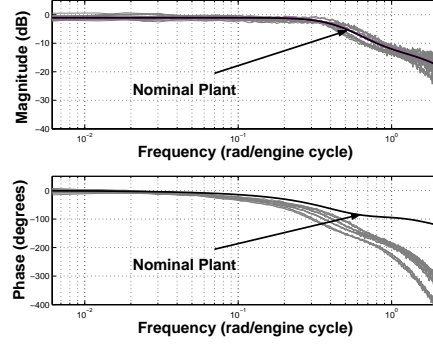


Figure 2: System Identification of Engine Torque.

A nominal plant transfer function,

$$P_o(s_\theta) = \frac{0.885 \left(\left(\frac{s_\theta}{0.911} \right)^2 + \frac{2(0.707)}{0.911} s_\theta + 1 \right)}{\left(\left(\frac{s_\theta}{1.759} \right)^2 + \frac{2(0.707)}{1.759} s_\theta + 1 \right) \left(\left(\frac{s_\theta}{0.440} \right)^2 + \frac{2(0.707)}{0.440} s_\theta + 1 \right)} \quad (5)$$

was developed using the experimental frequency responses shown in Figure 2. The nominal plant transfer function was chosen such that the magnitude of its frequency response is approximately equal to the mean of the experimental frequency response magnitudes for each frequency. It is clear from the system frequency response functions that a pure delay exists. Now that a nominal plant has been determined, the nonlinearities and uncertainty must be incorporated into the model.

For this design, multiplicative uncertainty was chosen to capture the system nonlinearities and delay (additive uncertainty could have been chosen). Multiplicative uncertainty may be written as

$$P = (1 + \Delta \hat{W}_2) P_o \quad (6)$$

where P is the perturbed plant, P_o is the nominal plant, \hat{W}_2 is a fixed stable transfer function (minimum uncertainty weighting function based on experimental frequency response functions), and Δ is a variable stable transfer function satisfying

$$\|\Delta\|_\infty \leq 1. \quad (7)$$

The minimum uncertainty weighting function based on experimental frequency response functions, incorporating the pure delay, may be determined by the following expression,

$$\left| \frac{P(j\omega_\theta)}{P_o(j\omega_\theta)} - 1 \right| \leq |\hat{W}_2(j\omega_\theta)|, \quad \forall \omega_\theta. \quad (8)$$

This is discussed by Doyle [13]. An illustration of the minimum uncertainty weighting function based on experimental frequency response functions using multiplicative uncertainty is shown in Figure 3.

2.2 H_∞ Torque Controller Design

Now that the steady state torque function and engine torque have been identified, the H_∞ torque controller may now be

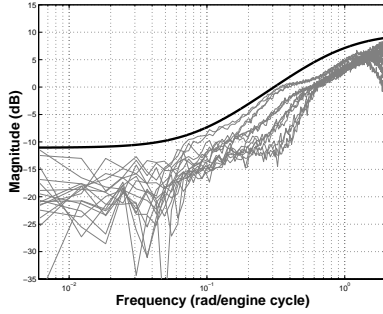


Figure 3: Uncertainty of Engine Torque Identification.

synthesized. The closed loop torque control block diagram may be written as shown in Figure 4. The input (w) is the torque disturbance, output (z) is the actual output torque, (e) and (u) are the controller input and output respectively, and finally (q) and (p) are the uncertainty input and output respectively. The performance weighting function is W_1 , W_2 is the uncertainty weighting function, and K is the H_∞ controller.

The general framework considered for H_∞ controller design is shown in Figure 5. As defined by Equation (7), the norm of the uncertainty, $\|\Delta\|_\infty$, is less than or equal to unity. Therefore the H_∞ controller design seeks to find a controller K such that the system is stable and minimizes the H_∞ norm of the transfer function from w to z . The system block diagram shown in Figure 4 may be manipulated into the general H_∞ framework shown in Figure 5. Once this is complete, an H_∞ controller may be designed using standard methods. More information concerning the standard H_∞ controller design methodology may be found in Zhou [14] and Chiang [15].

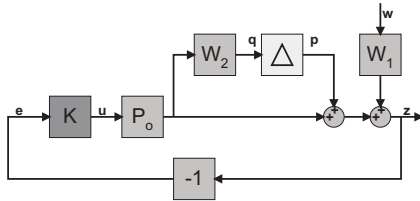


Figure 4: Block Diagram of Torque Control System.

2.2.1 Weighting Function Selection: Closed loop system performance is contingent upon the choice of weighting functions. The selection of weighting functions is often difficult. However, there exist general guidelines for developing weighting functions. The choice of weighting functions and how each relates to engine control systems are given in Carnevale [16], Williams [17], and Chiang [15]. More advanced techniques for selecting weighting functions exist, such as a method developed by Franchek for selecting weighting functions to enforce time domain tolerances [18]. This is by no means a complete list of references regarding this subject. In general, the more weighting func-

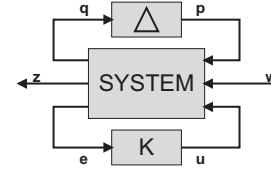


Figure 5: General System Interconnection.

tion dynamics, i.e. poles and zeros, the larger order controller [16]. Therefore, in a sense, the choice of weighting functions is constrained by order. However, if required, controller order reduction techniques exist to determine reduced order controllers with little sacrifice to performance. The following subsections will discuss the selection of weighting functions for our application.

Determination of the Uncertainty Weighting Function: The uncertainty weighting function, W_2 , defines how much is really known about the system for controller design and may also be manipulated to produce the desired closed loop system response. Equation (8) is implemented to determine the minimum uncertainty weighting function based on experimental frequency response functions, \hat{W}_2 . The uncertainty weighting function for this controller design is

$$W_2(s_\theta) = 0.43 \cdot \frac{\frac{s_\theta}{0.1} + 1}{\frac{s_\theta}{22} + 1} \quad (9)$$

where

$$|W_2(j\omega_\theta)| \geq |\hat{W}_2(j\omega_\theta)|, \forall \omega_\theta \quad (10)$$

must be satisfied. The frequency response of W_2 is illustrated in Figure 6.

Determination of the Performance Weighting Function: The performance weighting function, W_1 , can be used to selectively emphasize (and de-emphasize) various frequency ranges of interest from the point of view of closed loop performance. The performance weighting for this design,

$$W_1(s_\theta) = \frac{0.0249}{\left(\frac{s_\theta}{20.106}\right)^2 + \frac{2(0.707)}{20.106}s_\theta + 1}, \quad (11)$$

is chosen to weigh the low frequency content of the disturbance torque more than the higher frequency content. Essentially, this requires the H_∞ controller to minimize the error around lower frequencies at the cost of error around higher frequencies. The frequency response of W_1 is illustrated in Figure 6. The determination of the weighting functions for H_∞ controller design may be somewhat intuitive, however choosing the proper weighting functions to achieve an "optimal" system performance is by trial and error.

2.2.2 Robust Torque Controller Design: One of the system requirements of this controller design is the closed loop system must have a zero steady state error. This requires the controller to have one free integrator. Since

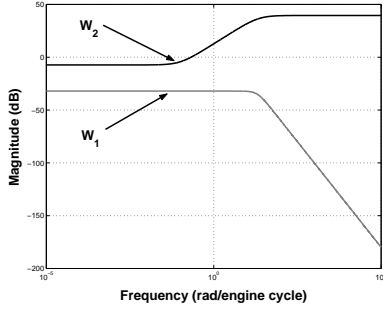


Figure 6: Weighting Functions for Controller Design.

the H_∞ controller design is a synthesis technique, the designer cannot directly dictate the location of certain poles and zeros of the controller. To incorporate a free integrator into the design, the nominal plant transfer function was augmented with a free integrator and gain during the controller synthesis. The H_∞ torque controller was determined using the *hinflmi* command in MATLAB[®]¹. The final controller was achieved after several design iterations. The design iterations consist of weighting function modifications, specifically the placement of pole(s)/zero(s) and gain of W_1 and W_2 , until the desired closed loop response is achieved via simulations. The final weighting functions are given in Equations (9) and (11).

Simulations of disturbances were implemented using MATLAB[®] and Simulink[®]. Three plant transfer functions with pure delays were simulated for each case. An upper and lower bound on the experimental frequency response functions, shown in Figure 2, as well as the nominal plant were considered during simulations. The transfer functions based on the upper and lower bounds of the frequency response functions shown in Figure 2 were not explicitly a part of the uncertainty considered via \hat{W}_2 , but merely extreme possibilities of the plant dynamics to test the robustness of the controller.

After the design was complete, a balanced truncation method was employed to reduce the order of the controller. The reduced order controller, with the free integrator and gain that previously augmented the plant during the design, was then converted to the discrete domain. The final discrete controller is

$$K(z_\theta^{-1}) = \frac{0.0101 + 0.01458z_\theta^{-1} - 0.003012z_\theta^{-2} - 0.01122z_\theta^{-3} - 0.005795z_\theta^{-4} - 0.002287z_\theta^{-5} - 0.0002182z_\theta^{-6}}{1 - 0.1327z_\theta^{-1} - 2.473z_\theta^{-2} - 0.2262z_\theta^{-3} - 2.056z_\theta^{-4} - 0.09959z_\theta^{-5} - 0.5773z_\theta^{-6}} \quad (12)$$

where the sampling period is 90 crank degrees and the subscript, θ , denotes the controller is implemented in the crank-

¹MATLAB and Simulink are registered trademarks of MathWorks, Inc. of Natick Massachusetts

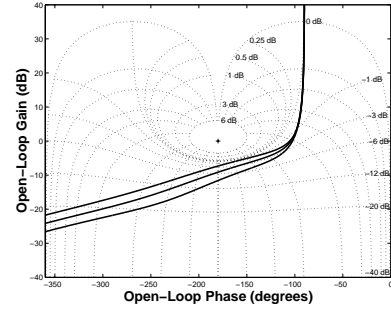


Figure 7: Nichols Chart of Torque Control System.

angle domain. A Nichols chart describing the closed loop system response for this controller, with each of the three plants considered during simulations, is shown in Figure 7. The three frequency response functions lie close to the 0 dB contour suggesting the final design should not overshoot and/or oscillate. Furthermore, responses to higher frequencies are attenuated as denoted by the amplitude roll off.

2.2.3 Experimental Validation of the Torque Controller: The H_∞ torque controller was implemented in real time via dSpace and an engine dynamometer. A block diagram of the implementation is provided in Figure 8. Engine speed and torque conditions for 25, 47, 58, and 74 mph, as specified in Table 1, were investigated.

Results of the torque controller for λ disturbances are shown in Figure 9. In this case, the engine operating condition was set to 25, 47, 58, and 74 mph and λ was stepped between 0.7 and 1.3. The torque was recorded using a load cell filtered at 25 Hz. For the worst case, torque variations were 9.1 percent of nominal.

In this particular case, a likely cause of the torque variations is the poor extension of spark timing beyond stoichiometry. Haider [19] demonstrated that reducing spark advance can lead up to a 40 percent torque reduction. Poor spark timing would cause an aggravated torque disturbance during an AFR shift and therefore demand more intervention from the torque controller. Better information concerning spark timing would mitigate torque disturbances to the system and improve overall system performance. In addition to spark timing, another likely cause is an improper coordination of air and fuel to the cylinder. The controller provided zero steady state error and an acceptable response on the dynamometer to the torque disturbances. However, vehicle testing must be completed to ensure these results meet vehicle drivability standards.

The torque controller may also be implemented to change desired torque. Again, engine conditions for 25, 47, 58, and 74 mph were investigated. In this case, desired engine torque was stepped while operating at $\lambda = 0.7$, $\lambda = 1.0$, and $\lambda = 1.3$. In many conditions, the engine responded to a 20 ft-lb step change in desired torque within 12 to 34 engine cy-

cles. If required, an increase in transient performance may be provided by the design of an appropriate prefilter. An advantage of the robust controller methodology employed for this design is the fact the system, in general, responds well over a large operating range despite the system nonlinearities.

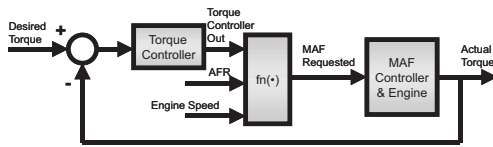


Figure 8: Overall Block Diagram.

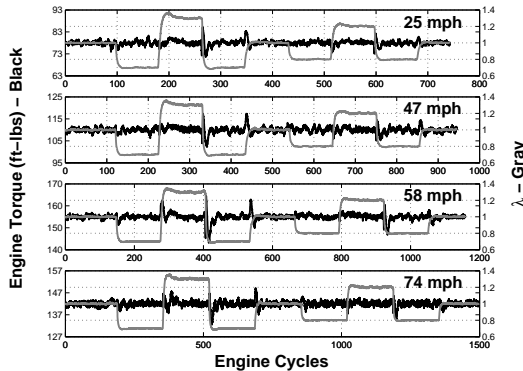


Figure 9: System Performance Stepping Lambda at Various Engine Conditions.

3 Conclusions

In this paper a robust controller design procedure was presented for the regulation of engine torque. The methodology consisted of two parts: (1) the identification of the open loop system and (2) an H_∞ robust controller design. To demonstrate this procedure, a 4.6L V8 spark ignition engine torque model was experimentally determined. In addition, a crank-angle domain H_∞ controller was designed to control engine torque with zero steady state error while incorporating system nonlinearities and a pure delay. In the worst dynamometer test cases with disturbances due to engine AFR, torque variations were 9.1 percent of nominal. To address vehicle drivability concerns, the controller must be validated via driver evaluations. The torque disturbances may be reduced using the same controller design methodology outlined in this investigation by taking into account spark timing and EGR. In addition, disturbances may be mitigated by better open loop coordination of spark timing, fuel, mass air flow, and EGR.

References

[1] T. Inoue, K. Aoki, and T. Suzuki. Future engine control. Technical Report 901152, SAE, 1990.
 [2] A. Stefanopoulou, J. Grizzle, and J. Freudenberg. Engine air-fuel ratio and torque control using secondary throttles. *Proceedings of the IEEE Conference on Decision and Control*, 3:2748–53, 1994.

[3] S. Ginoux and J. Champoussin. Engine torque determination by crankangle measurements: State of the art, future prospects. Technical Report 970532, SAE, 1997.
 [4] P. Azzoni, D. Moro, F. Ponti, and G. Rizzoni. Engine and load torque estimation with application to electronic throttle control. Technical Report 980795, SAE, 1998.
 [5] E. Kamei, H. Namba, K. Osaki, and M. Ohba. Application of reduced order model to automotive engine control system. *Proceedings of the American Control Conference*, pages 1815–1820, 1987.
 [6] I. Kolmanovsky, J. Sun, and L. Wang. Coordinated control of lean burn gasoline engines with continuously variable transmissions. *Proceedings of the American Control Conference*, pages 2673–2677, 1999.
 [7] A. Balluchi, A. Bicchi, C. Caterini, C. Rossi, and A. Sangiovanni-Vincentelli. Hybrid tracking control for spark-ignition engines. *Proceedings of the 39th IEEE Conference on Decision and Control*, pages 3126–3131, 2000.
 [8] S. Billings, S. Chen, and M. Korenberg. Identification of MIMO non-linear systems using a forward-regression orthogonal estimator. *International Journal of Control*, 49(6):2157–2189, 1989.
 [9] C. Taylor. *The Internal-Combustion Engine in Theory and Practice*, volume 1. The M.I.T. Press, 2nd edition, 1977.
 [10] G. Ingram, M. Franchek, and V. Balakrishnan. Spark ignition engine mass air flow control for precise torque management. Technical Report 2003-01-0624, SAE, 2003.
 [11] Y. Chin and F. Coats. Engine dynamics: Time-based versus crank-angle based. Technical Report 860412, SAE, 1986.
 [12] J. Bendat and A. Piersol. *Engineering Applications of Correlation and Spectral Analysis*. John Wiley and Sons, Inc., 2nd edition, 1993.
 [13] J. Doyle, B. Francis, and A. Tannenbaum. *Feedback Control Theory*. Macmillan Publishing Co., 1992.
 [14] K. Zhou, J. Doyle, and K. Glover. *Robust and Optimal Control*. Prentice Hall, 1996.
 [15] R. Chiang and M. Safonov. *Robust Control Toolbox, User's Guide*. The Math Works, Inc., 1997.
 [16] C. Carnevale and A. Moschetti. Idle speed control with H-infinity technique. Technical Report 930770, SAE, 1993.
 [17] S. Williams, D. Hrovat, C. Davey, D. Maclay, J. Crevel, and L. Chen. Idle speed control design using an H-infinity approach. *Proceedings of the American Control Conference*, 3:1950–56, 1989.
 [18] M. Franchek. Selecting the performance weights for mu and H-infinity synthesis methods for SISO regulating systems. *Transactions of the ASME*, 118:126–31, 1996.
 [19] S. Haider and J. Griffin. Powertrain torque management. Technical Report 870081, SAE, 1987.